THE JOURNAL OF BIOLOGICAL CHEMISTRY VOL. 287, NO. 19, pp. 15489–15501, May 4, 2012

Transcriptional Regulation of T-type Calcium Channel $Ca_V3.2$

BI-DIRECTIONALITY BY EARLY GROWTH RESPONSE 1 (Egr1) AND REPRESSOR ELEMENT 1 (RE-1) PROTEIN -SILENCING TRANSCRIPTION FACTOR (REST)[*] [S]

Received for publication, October 5, 2011, and in revised form, February 29, 2012 Published, JBC Papers in Press, March 19, 2012, DOI 10.1074/jbc.M111.310763

Karen M. J. van Loo[‡1], **Christina Schaub**[§¶], **Katharina Pernhorst**[‡], **Yoel Yaari**[‖], **Heinz Beck**[§**], **Susanne Schoch**[‡], **and Albert J. Becker**[‡]

From the Departments of [‡]*Neuropathology,* [§]*Epileptology, and* [¶]*Neurology, University of Bonn Medical Center, D-53105 Bonn, Germany, the* [‖]*Department of Medical Neurobiology, Institute for Medical Research Israel-Canada, Hebrew University-Hadassah School of Medicine, Jerusalem 91120, Israel, and* **Deutschen Zentrum für Neurodegenerative Erkrankungen, D-53175 Bonn, Germany*

Background: Expression of the T-type Ca^{2+}-channel $Ca_V3.2$ has to be tightly regulated for proper calcium homeostasis.
Results: Overexpression of the transcription factor Egr1 strongly activates the *$Ca_V3.2$* promoter and can be counteracted by the repressor REST.
Conclusion: Egr1 and REST "bi-directionally" regulate the *$Ca_V3.2$* promoter.
Significance: Our results have important implications for calcium homeostasis and dynamics in health and disease.

The pore-forming Ca^{2+} channel subunit $Ca_V3.2$ mediates a low voltage-activated (T-type) Ca^{2+} current (I_{CaT}) that contributes pivotally to neuronal and cardiac pacemaker activity. Despite the importance of tightly regulated $Ca_V3.2$ levels, the mechanisms regulating its transcriptional dynamics are not well understood. Here, we have identified two key factors that up- and down-regulate the expression of the gene encoding $Ca_V3.2$ (*Cacna1h*). First, we determined the promoter region and observed several stimulatory and inhibitory clusters. Furthermore, we found binding sites for the transcription factor early growth response 1 (Egr1/Zif268/Krox-24) to be highly overrepresented within the *$Ca_V3.2$* promoter region. mRNA expression analyses and dual-luciferase promoter assays revealed that the *$Ca_V3.2$* promoter was strongly activated by Egr1 overexpression *in vitro* and *in vivo*. Subsequent chromatin immunoprecipitation assays in NG108-15 cells and mouse hippocampi confirmed specific Egr1 binding to the *$Ca_V3.2$* promoter. Congruently, whole-cell I_{CaT} values were significantly larger after Egr1 overexpression. Intriguingly, Egr1-induced activation of the *$Ca_V3.2$* promoter was effectively counteracted by the repressor element 1-silencing transcription factor (REST). Thus, Egr1 and REST can bi-directionally regulate *$Ca_V3.2$* promoter activity and mRNA expression and, hence, the size of I_{CaT}. This mechanism has critical implications for the regulation of neuronal and cardiac Ca^{2+} homeostasis under physiological conditions and in episodic disorders such as arrhythmias and epilepsy.

Low voltage-activated (T-type) Ca^{2+} channels are expressed in multiple organs, including the CNS and heart (1–4), where they play a key role in many cellular processes, such as shaping of neuronal discharge patterns, secretion of hormones and neurotransmitters, amplification of dendritic excitatory postsynaptic potentials, maintenance of circadian rhythms, and pacing of the heart (4–6). T-type Ca^{2+} channels comprise a subfamily of three Ca_V3 pore-forming channel subunits ($Ca_V3.1$, $Ca_V3.2$, and $Ca_V3.3$), encoded by members of the *Cacna1* gene family (*Cacna1g*, *Cacna1h*, and *Cacna1i*). The common biophysical characteristics of these three Ca_V3 channel subtypes are activation at subthreshold voltages, comparatively slow activation and deactivation kinetics, and complete inactivation during a sustained depolarization (7). In addition to their common characteristics, the Ca_V3 channels also exhibit diverging properties. $Ca_V3.3$ channels display particularly slow inactivation kinetics, and $Ca_V3.2$ channels are significantly more sensitive to nickel than $Ca_V3.1$ and $Ca_V3.3$ (6, 8–10).

The importance of T-type Ca^{2+} channels for normal cellular function is underscored by the pathophysiological alterations associated with genetic and acquired *$Ca_V3.2$* "channelopathies." Gain-of-function mutations in the *$Ca_V3.2$* gene are associated with idiopathic generalized/absence epilepsy (11–13). Likewise, acquired increases in thalamic and hippocampal *$Ca_V3.2$* expression contribute to the development of chronic epilepsy (14, 15). In addition, overexpression of $Ca_V3.2$ channels in myocytes may result in the development of several cardiac dysfunctions, including ventricular arrhythmias (16, 17). Epileptic seizures as well as cardiac arrhythmias share the episodic onset of symptoms. Because no overlapping mutations for both conditions have been identified in *$Ca_V3.2$*, transcriptionally mediated changes in *$Ca_V3.2$* levels might constitute an attractive mechanism explaining the common episodic onset. However, despite the importance and potency of transcriptional regulation, only little is known about the key mechanisms controlling expression of the *$Ca_V3.2$* gene. Recently, an intriguing transcriptional

* This work was supported by Deutsche Forschungsgemeinschaft (SFB/TR3, KFO 177, SFB-645; to A. J. B., Y. Y., H. B., and S. S.), GIF (to A. J. B., S. S., and Y. Y.), NGFNplus EMINET (to A. J. B., H. B., and S. S.), European Union EPICURE (to A. J. B. and H. B.), Euroepinomics Network of the European Science Foundation (to K. v L. and A. J. B.), Else Kröner-Fresenius-Stiftung (to A. J. B.), and BMBF "Independent research groups in neurosciences" (to S. S.) as well as the BONFOR program of the University of Bonn Medical Center.
[S] This article contains supplemental Figs. 1 and 2.
[1] To whom correspondence should be addressed: Dept. of Neuropathology, University of Bonn Medical Center, Sigmund-Freud Str. 25, D-53105 Bonn, Germany. Tel.: 49-228-287-19346; E-mail: karen.van_loo@ukb.uni-bonn.de.

mechanism of T-type Ca^{2+} channel regulation has been described. Repressor element-1 (RE-1)[2]-silencing transcription factor (REST, also known as NRSF (neuron-restrictive silencer factor)) was found to function as a transcriptional regulator of $Ca_V3.2$ in the heart of mice (16, 18). REST was originally described as a repressor of neuronal gene expression and can bind to a neuron-restrictive silencer element in the genome, also known as RE-1. Although its levels are generally low, neuronal REST expression is up-regulated after extended periods of neuronal hyperactivity, as demonstrated after seizures, neuropathic pain, and ischemia (19–22).

Here, we have used bioinformatic and molecular approaches to characterize the *$Ca_V3.2$* promoter in detail and to identify potential mechanisms regulating *$Ca_V3.2$* transcription. Our analyses show for the first time that the transcription factor early growth response 1 (Egr1/Zif268/Krox-24) mediates *$Ca_V3.2$* promoter activation. Moreover, this effect of Egr1 is potently antagonized by the transcriptional repressor REST. The functional interactions described here may have important implications for *$Ca_V3.2$* regulation under physio- and pathological conditions.

EXPERIMENTAL PROCEDURES

Bioinformatic Analysis—The genomic sequence of the rat *$Ca_V3.2$* gene was obtained from the UCSC genome browser. Potential transcription start sites were identified using the Eponine software (threshold value of 0.99) (23). Comparative analysis of the nucleotides of the *$Ca_V3.2$* gene of different species was performed with PhyloP (PHAST package) and Vector NTI (9.0) using default parameters. Potential transcription factor (TF) binding sites were identified using the MathInspector RegionMiner software tool (Genomatix).

Cloning and Plasmids—The mammalian expression vectors pCMV-Egr1, pCMV-myc-REST and pCMV-FLAG-NLS-$REST_{DBD}$ were kindly provided by Prof. Gerald Thiel (University of Saarland Medical Center, Homburg, Germany).

The rat full-length *$Ca_V3.2$*−1426 promoter region was amplified by PCR using rat genomic DNA as template with the primer set forward (MluI) (5′-GCG ACG CGT AAG GGA TAA GGG TCA TGT AAC CAC T-3′) and reverse (XhoI) (5′-GCG CTC GAG GAG AGA GGG CAG GAG GT-3′) and subcloned into the MluI-XhoI-digested luciferase reporter vector pGL-3 basic (Promega Biotech, Madison, WI). Generation of the rat deletion fragments (Figs. 2*C* and 4*A*) was achieved by PCR with the same reverse primer as used to amplify full-length *$Ca_V3.2$*−1426 and the following forward primers: *$Ca_V3.2$*−1188, 5′-CAA TTG GTG TCG CGT CGC GCA T-3′; *$Ca_V3.2$*−1020, 5′-CAG TGA AGG GAA GGG GCG GCG C-3′; *$Ca_V3.2$*−947, 5′-GGG AAG GAC GTT GGC GCC GC-3′; *$Ca_V3.2$*−312, 5′-ATG CCC ACG GGG ACG C-3′; *$Ca_V3.2$*−280, 5′-GAG GTG AGA TGC GGA GGG TAC G-3′; *$Ca_V3.2$*−105, 5′-GAG ACA AAG ACA TCC CGG CG-3′. All forward primers contained a 5′-GCGACGCGT-MluI overhang for subcloning into the pGL-3 basic vector. The *$Ca_V3.2$*−1426-REST reporter plasmid was cloned by ligating a BamHI-SalI-digested rat genomic PCR fragment (forward, 5′-GCG GGA TCC ACT CTG CTC TAA TGA GGG ACC CT-3′; reverse, 5′-GCG GTC GAC GCT ACC CCA CGG CAA GGT-3′) into the pGL3-*$Ca_V3.2$*−1426 vector digested with BamHI and SalI. For construction of the pAAV-Synapsin-Egr1-IRES-Venus plasmid, pAAV-Syn-IRES-Venus (kindly provided by Martin Schwarz, Heidelberg, Germany) was modified. The Egr1 sequence was amplified from pCMV-Egr1 using the primers: forward (NheI) (5′-GCG GCT AGC CCG CCA CCA TGG CAG CG-3′) and reverse (BamHI) (5′- GCG GGA TCC CCC TTT AGC AAA TTT CAA TTG TCC-3′) and cloned in the NheI-BamHI-digested pAAV-Syn-IRES-Venus vector. The correctness of the plasmids was confirmed by sequencing analyses.

Cell Culture, Transfections, and Luciferase Assays—NG108-15 cells were maintained at 37 °C and 5% CO_2 in Dulbecco's modified Eagle's medium (DMEM) supplemented with 10% (v/v) heat-inactivated fetal calf serum (Hyclone), 100 units/ml penicillin/streptomycin, 2 mM glutamine, and 1× HAT (sodium hypoxanthine, aminopterin, and thymidine; Invitrogen). Transfection was performed in 48-well tissue culture plates (80% confluency) using Lipofectamine (Invitrogen) following the manufacturer's protocol. Briefly, 0.05 μg of *$Ca_V3.2$* luciferase reporter plasmid with firefly luciferase and 0.0125 μg of control pRL-TK vector with the *Renilla* luciferase gene (Promega) together with the amount of overexpression plasmids as indicated were mixed with 25 μl of Opti-MEM medium (Invitrogen). The mixture was incubated for 20 min at room temperature and then added to the appropriate wells. Cells were grown in serum-free culture medium at 37 °C and 5% CO_2. After 12 h, the serum-free medium was replaced by serum containing medium. The cells were collected 48 h after transfection. The luciferase assay was performed using the Dual Luciferase Reporter Assay System (Promega) according to the manufacturer's specifications. *Renilla* and firefly luciferase activities were determined using the Glomax Luminometer (Promega). The results are given as firefly/*Renilla* relative light units.

RT-PCRs—mRNA was isolated with a Dynabeads mRNA Direct Micro kit (Invitrogen) according to the manufacturer's protocol, and first-strand cDNA was prepared using RevertAid Reverse Transcriptase (Fermentas). The presence of *$Ca_V3.2$* , *Egr1*, *REST*, and the truncated *REST4* variant was analyzed by RT-PCR. PCR samples contained 1× GoTaq buffer (Promega), 2.5 mM $MgCl_2$, 0.1 mM each of dTTP, dATP, dCTP, and dGTP, 0.5 units of GoTaq (Promega), 10 pmol each oligonucleotide primer (Invitrogen), and 1/20 synthesized cDNA in a 25-μl volume. The following primers were used: *$Ca_V3.2$* forward (5′-ATG TCA TCA CCA TGT CCA TGG A-3′); *$Ca_V3.2$* reverse (5′-ACG TAG TTG CAG TAC TTA AGG GCC-3′); *Egr1* (forward, 5′-GGA GCC GAG CGA ACA ACC CT-3′); *Egr1* reverse (TCC AGG GAG AAG CGG CCA GT-3′); *REST* and *REST4* forward (5′-AGC GAG TAC CAC TGG AGG AAA CA-3′); *REST* reverse (5′-AAT TAA GAG GTT TAG GCC CGT TG-3′); *REST4* reverse (5′-ATA CCC AGC TAG ATC ACA CT-3′). PCR was performed with conditions as follows: 2 min at 94 °C, then 30 cycles of 45 s at 94 °C, 30 s at 60 °C, and 45 s at 72 °C followed by a final extension step at 72 °C for 10 min. PCR

[2] The abbreviations used are: RE-1, repressor element-1; REST, RE-1-silencing transcription factor; Egr1, early growth response 1; TF, transcription factor; PI, protease inhibitor; rAAV, recombinant adeno-associated virus; ANOVA, analysis of variance; ERE, Egr1 responsive element; SE, status epilepticus.

products were analyzed on a 2% agarose gel. A control (no template) was included for each primer set.

Quantitative Real Time RT-PCR—Transcript quantification was performed by quantitative real time RT-PCR analysis according to the $\Delta\Delta C_t$ method. β-Actin was amplified from all samples to normalize expression. Quantitative RT-PCR was performed in a 6.25-μl reaction volume containing 3.125 μl of Maxima SYBR Green/Rox qPCR Master Mix (Fermentas), 1.5 μl of diethyl pyrocarbonate H_2O, 1.25 μl of cDNA, and 0.1875 μl of each primer (10 pmol/ml; *$Ca_V3.2$* and *Egr1*, same primers as described above; β-actin forward, 5′-CGT GAA AAG ATG ACC CAG ATC A-3′; β-actin reverse, 5′-GGA CAG CAC AGC CTG GAT G-3′). Reactions were performed in triplicate. After preincubation for 10 min at 94 °C, 40 PCR cycles (20 s at 94 °C, 30 s at 59 °C, and 40 s at 72 °C) were performed on an ABI Prism 9700HT system (PE Applied Biosystems, Foster City, CA).

Chromatin Immunoprecipitation (ChIP) Assays-ChIP on Cultured Cells—NG108-15 cells (6 wells; 80% confluency) were transiently transfected with pCMV-Egr1 or the empty pCMV vector (0.4 μg/well) using Lipofectamine as described above. 48 h after transfection the cells were cross-linked in DMEM with 1% formaldehyde for 10 min at 37 °C. Cells were washed twice in cold PBS containing protease inhibitors (PIs; Complete Protease Inhibitor Mixture Tablets; Roche Applied Science) and collected into conical tubes. Cells were spun down and lysed in 200 μl of SDS lysis buffer (1% SDS, 10 mM EDTA, 50 mM Tris, pH 8.1 with PIs) and incubated on ice for 10 min.

ChIP on Brain Tissue—Mice were decapitated under deep isoflurane anesthesia (Forene). Hippocampi were removed quickly, snap-frozen, and stored at −80 °C until further processing. 1% Formaldehyde was added to the tissue (200 μl/hippocampus), and the tissues were incubated for 10 min at 37 °C. Next, hippocampi were washed twice in cold PBS with PIs, suspended in 200 μl of SDS lysis buffer (1% SDS, 10 mM EDTA, 50 mM Tris, pH 8.1, with PIs), and incubated on ice for 10 min.

ChIP Sample Processing—After 10 min on ice, lysates (both NG108-15 cells and mice hippocampi) were sonicated using an Ultrasonic Processor UP50H (Hielscher Ultrasound Technology) with four sets of 10-s pulses at 50% of maximum power. This treatment yielded an average of 300–500-bp DNA fragments. Samples were centrifuged at 13.000 rpm for 10 min, and the cell supernatant was diluted 10-fold in ChIP dilution buffer (0.01% SDS, 1.1% Triton X-100, 1.2 mM EDTA, 16.7 mM Tris, pH 8.1, 167 mM NaCl with PIs). To reduce nonspecific background, samples were precleared for 30 min with salmon sperm DNA/protein A agarose-50% slurry (Millipore). Next, samples were incubated overnight at 4 °C with 5 μg of anti-Egr1 SC110 antibody (Santa Cruz) or anti-NRSF (H-290) SC25398x antibody (Santa Cruz). Rabbit-IgG incubations were included as control for the immunoprecipitation. Salmon sperm DNA/protein A-agarose, 50% slurry was then added for 1 h at 4 °C. Nonspecifically associated proteins and DNA were removed from the beads by sequentially washing with low salt washing buffer (20 mM Tris-HCl, pH 8.1, 150 mM NaCl, 2 mM EDTA, 0.1% SDS, 1% Triton X-100), high salt washing buffer (20 mM Tris-HCl, pH 8.1, 500 mM NaCl, 2 mM EDTA, 0.1% SDS, 1% Triton X-100), LiCl washing buffer (0.25 M LiCl, 1% Nonidet P-40, 1% deoxycholate, 1 mM EDTA, 10 mM Tris-HCl, pH 8.1), and twice with TE buffer (10 mM Tris, pH 8.1, 1 mM EDTA). Next, immunoprecipitation complexes were eluted from the beads with 1% SDS and 0.1 M $NaHCO_3$, and cross-links were reversed overnight at 65 °C by adding 20 μl of 5 M NaCl to 500 μl of eluates. Proteins were then digested by adding 20 μg of proteinase K (Sigma) for 1 h at 45 °C. DNA was recovered by phenol/chloroform extraction, ethanol-precipitated with glycogen as a carrier, and resuspended in 25 μl of water. The recovered DNA was analyzed by PCR with primers spanning the *$Ca_V3.2$* promoter region: Egr-ChIP (ChIP on cultured cells and brain tissue): ChIP1 forward, 5′-CTG TTC CCG CAG CTC CGC TC-3′; ChIP1 reverse, 5′-GTG CCC TCG GTC ATG GTG GC-3′; ChIP2 forward, 5′-CGC GCG AGA AAA GGA GGG GG-3′; ChIP2 reverse, 5′-GCT CGC AGG GAT GCT CGG G-3′; ChIP3 forward, 5′-GAA GGG AGA TTC AGC GAC AT-3′; ChIP3 reverse, 5′-CCA ATT GTA CTG GGG CAG TC-3′. REST-ChIP (ChIP on cultured cells) primers were: forward (5′-GAC CCT ACT CCC TGG TTT GC-3′) and reverse (5′-TAA AAA CCC CCT CAA TGC AG-3′); REST-ChIP (ChIP on brain tissue) forward (5′- AGG TGG GAC AAC TGC TTC AG-3′) and reverse (5′- GGA TCA TCT TCA ATG CAC CA-3′). PCR amplification in a 25-μl reaction included 1 μl of immunoprecipitated DNA, 0.1 mM each of deoxyribonucleotide triphosphate (dNTP), 10 pmol of each primer, 2.5 mM concentrations of a 10× Mg^{2+} reaction buffer and 0.5 unit of DNA Taq polymerase (Invitrogen). Reactions were amplified for 35 cycles at 94 °C for 30 s, 60 °C for 30 s, and 72 °C for 1 min followed by a final extension step at 72 °C for 10 min. PCR products were analyzed on 2% agarose gels and quantified using AIDA software.

Electrophysiology Recordings and Analysis—Patch clamp recordings were obtained from NG108-15 cells. Patch pipettes with a resistance of 3–4 megaohms were fabricated from borosilicate glass capillaries and filled with an intracellular solution containing 110 mM CsF, 20 mM tetraethylammonium, 2 mM $MgCl_2$, 10 mM HEPES, 11 mM EGTA, 5 mM ATP, and 0.5 mM GTP, pH 7.2, adjusted with CsOH, 300 mosmol. Patch clamp recordings were performed in an artificial cerebrospinal fluid (ACSF) bath solution containing 125 mM sodium methanesulfonate, 3 mM KCl, 1 mM $MgCl_2$, 5 mM $CaCl_2$, 4 mM 4-aminopyridine, 20 mM tetraethylammonium, 10 mM HEPES, 10 mM glucose (pH 7.4, 315 mosmol). Tight-seal, whole-cell recordings were obtained at room temperature (21–24 °C) according to standard techniques. Membrane currents were recorded using a patch clamp amplifier (Axopatch 200B, Axon Instruments, Union City, CA). Series resistance compensation was employed to improve the voltage-clamp control (>80%) so that the maximal residual voltage error did not exceed 1.5 mV. Voltage recordings were corrected online for a liquid junction potential of 10 mV. Whole-cell Ca^{2+} currents were elicited with depolarizing voltage steps to −10 mV. The magnitude of I_{CaT} was quantified as the transient component of the resulting current traces. The recorded current can be attributed to $Ca_V3.2$ as they were largely blocked by application of 100 μM Ni^{2+}.

Viral Vector Production—Recombinant AAV1/2 genomes were generated by large scale triple transfection of HEK293 cells. The adeno-associated virus (AAV)-Syn-Egr1-IRES-Venus plasmid, helper plasmids encoding rep and cap genes

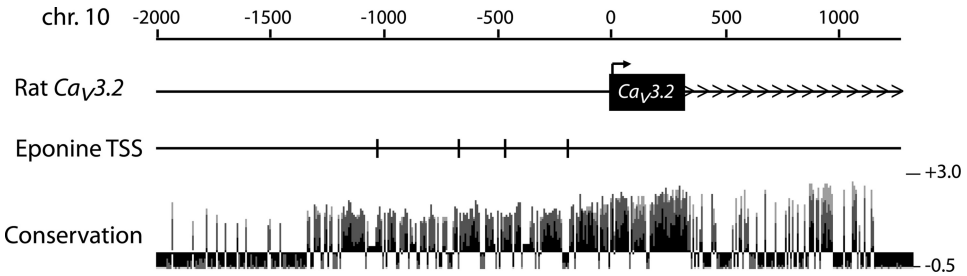

FIGURE 1. **Bioinformatic analysis of the rat *$Ca_V3.2$* promoter.** Shown is graphic representation of the 5′ region of the rat *$Ca_V3.2$* gene (chromosome (*chr.*) 10: 2000 nucleotides upstream and 1250 nucleotides downstream of the start ATG). Four predicted Eponine transcription start sites (*TSS*) and the level of conservation (based on PhyloP; Placental mammal base-wise conservation) are indicated. For the conservation scores, nucleotides predicted to be conserved are assigned positive scores, whereas nucleotides predicted to be fast-evolving are assigned negative scores.

(pRV1 and pH21), and adenoviral helper pFΔ6 (Stratagene) were transfected using standard $CaPO_4$ transfection. Cells were harvested ~60 h after transfection. Cell pellets were lysed in the presence of 0.5% sodium deoxycholate (Sigma) and 50 units/ml Benzonase endonuclease (Sigma). rAAV viral particles were purified from the cell lysate by HiTrap™ heparin column purification (GE Healthcare) and then concentrated using Amicon Ultra Centrifugal Filters (Millipore) until a final stock volume of 400 μl was reached. Purity of the viruses was validated by Coomassie Blue staining of SDS-polyacrylamide gels loaded with 7–15 μl virus stock.

Infusion of AAV vectors—Adult $Ca_V3.2^{+/+}$ mice (>60 days old; weight >20 g) were anesthetized with 6 mg/kg xylazine (Rompun; Bayer) plus 90–120 mg/kg ketamine, intramuscular (Ketavet; Pfizer). Intracerebral injection of viral particles in the left CA1 hippocampal region was performed stereotactically at the coordinates −2 posterior, −2 lateral, and 1.7 ventral relative to bregma. Holes the size of the injection needle were drilled into the skull, and 1 μl of viral suspension containing ~10^8 transducing units was injected using a 10-μl Hamilton syringe at a rate of 100 nl/min using a microprocessor controlled mini-pump (World Precision Instruments). After injection, the needle was left in place for 5 min before withdrawal. 14 Days after infection, mice were decapitated under deep isoflurane anesthesia (Forene), and hippocampi were removed. All experiments were performed in accordance with the guidelines of the University of Bonn Medical Center Animal Care Committee.

Statistical Analysis—Student's *t* tests and one-way ANOVA followed by Bonferroni's multiple comparison tests were used to evaluate the statistical significance of the results. Values were considered significantly at $p < 0.05$. All results are plotted as the mean ± S.E.

RESULTS

Bioinformatic Prediction of $Ca_V3.2$ Promoter Region—To determine key molecular mechanisms underlying *$Ca_V3.2$* expression control, we first aimed to identify the *$Ca_V3.2$* promoter region using bioinformatics. The sequence upstream of the translation start site of the rat *$Ca_V3.2$* gene was analyzed for the presence of promoter region characteristics including transcription start sites and a high level of conservation between species. By using the Eponine software tool, four transcription start sites were found within the upstream region of the *$Ca_V3.2$* gene, located 183, 467, 695, and 1064 bp upstream of the start ATG (Fig. 1). Furthermore, conservation analysis of the upstream *$Ca_V3.2$* gene showed a high degree of homology throughout the first exon (80% identity between rat, mouse, and human) and within the first 700 bp upstream of the start ATG (>65% identity). A gradual decrease in sequence homology was observed for the more upstream sequences, with a sequence homology of less than 60% 1400 bp upstream of the start ATG (Fig. 1). Based on our bioinformatic analysis, we hypothesized that the 1400 nucleotides upstream of the start ATG contain the major regulatory promoter elements.

In Vitro Delineation of $Ca_V3.2$ Promoter Region—We next examined whether the bioinformatically predicted *$Ca_V3.2$* promoter region is indeed sufficient for basal activity in neuronal cells. For this, we selected NG108-15 neural cells, which express *$Ca_V3.2$* mRNA under naïve conditions (Fig. 2*A*). We cloned the predicted full-length rat *$Ca_V3.2$* promoter region (*$Ca_V3.2$*−1426) into a firefly luciferase reporter plasmid and measured reporter activity in transiently transfected NG108-15 cells. Luciferase activity of the *$Ca_V3.2$* promoter was ~8-fold higher than the pGL3 control plasmid, which lacks a promoter (Fig. 2*B*), suggesting that this region of the *$Ca_V3.2$* gene has significant promoter activity.

To pinpoint the exact region responsible for *$Ca_V3.2$* promoter activation and to identify potential stimulatory and inhibitory regions, NG108-15 cells were transiently transfected with *$Ca_V3.2$* deletion reporter constructs (*$Ca_V3.2$*−1188, −1020, −947, −312, −280, and −105). Each deletion fragment was tested multiple times with either three or four wells per construct and using two independent DNA isolations per construct. The basal activity of the first deletion fragment (*$Ca_V3.2$*−1188) was significantly lower ($p \leq 0.001$) than the activity of the full-length *$Ca_V3.2$*−1426 construct (Fig. 2*C*), suggesting the presence of stimulatory elements in the 238 nucleotides upstream of the *$Ca_V3.2$*−1188 fragment. The activity of the second deletion fragment (*$Ca_V3.2$*−1020) was as high as that of full-length *$Ca_V3.2$*−1426, indicating the presence of an unknown repressor(s) in the 168 nucleotides upstream of the *$Ca_V3.2$*−1020 fragment. Moreover, the two subsequent deletion fragments (*$Ca_V3.2$*−947 and *$Ca_V3.2$*−312) again showed a reduced basal activity, comparable with the basal activity of the *$Ca_V3.2$*−1188 fragment, whereas the basal activity of the two smallest deletion fragments (*$Ca_V3.2$*−280 and *$Ca_V3.2$*−105) was again at the level of the basal activity of the full-length construct (*$Ca_V3.2$*−1426). These results indicate that several stimulatory and inhibitory regulatory elements are spread

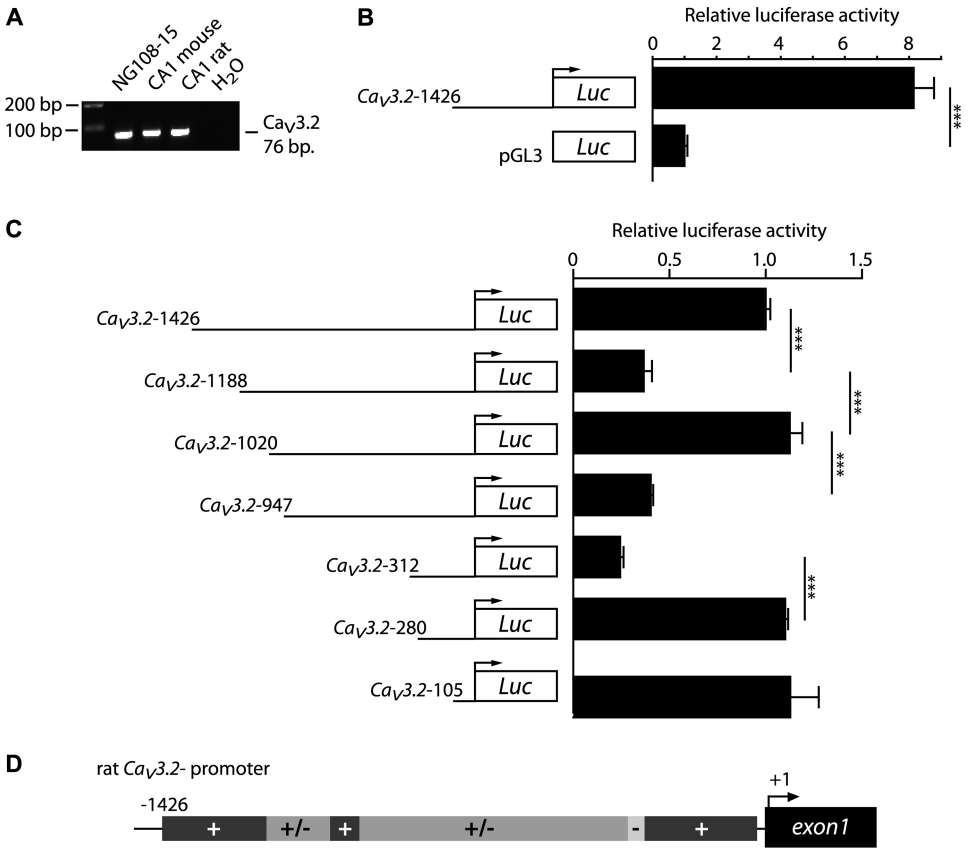

FIGURE 2. **The predicted $Ca_V3.2$ promoter region contains functional regulatory elements.** *A*, $Ca_V3.2$ mRNA expression analysis in NG108-15 cells and hippocampal CA1 region of mouse and rat using RT-PCR is shown. *B*, basal activity of the predicted $Ca_V3.2$ promoter construct ($Ca_V3.2-1426$) in NG108-15 cells is shown. Activity of the $Ca_V3.2-1426$ luciferase construct is ~8 times stronger than the activity of the promoterless pGL3 vector (*t* test; ***, $p \leq 0.001$; $n = 4$). *C*, basal luciferase activity of the $Ca_V3.2$ promoter deletion fragments is shown. Note the significantly lower luciferase activity of the $Ca_V3.2-1188$, $Ca_V3.2-947$, and $Ca_V3.2-312$ deletion fragments, indicating the presence of unknown repressors or lack of activators in those fragments (one-way ANOVA: ***. $p \leq 0.001$; $n \geq 3$). *D*, shown is a schematic overview of the stimulatory (+) and inhibitory (−) elements located in the rat $Ca_V3.2$ promoter region.

throughout the entire predicted $Ca_V3.2$ promoter region and that *in vitro* all seven $Ca_V3.2$ deletion fragments exhibit promoter activity (Fig. 2*D*). Furthermore, the strong promoter activity of the smallest $Ca_V3.2-105$ fragment suggests that this fragment functions as the $Ca_V3.2$ core promoter.

Identification of Putative Transcription Factor Binding Sites in $Ca_V3.2$ Promoter Region—To identify potential regulatory mechanisms underlying $Ca_V3.2$ expression, we first aligned the bioinformatically predicted rat $Ca_V3.2$ promoter region with genomic $Ca_V3.2$ sequences of mouse and human. The homologous sequences of rat (1464 nucleotides upstream from the start ATG), mouse (1468 nucleotides), and human (1597 nucleotides) were analyzed for the presence of enriched TF binding sites using the Genomatix RegionMiner software tool. TF binding sites were ranked based on their overrepresentation value calculated against either the whole genome (Z-score genome) and all annotated promoter regions of the genome (Z-score promoter). For the predicted rat $Ca_V3.2$ promoter region, 255 different TF matrices were found with the highest Z-score genome for Egr1 followed by zinc finger protein 161 (ZFP161 also known as ZF5) and Sp4 transcription factor (SP4) (Table 1). The highest Z-score promoter was also found for Egr1 followed by SP4 and zinc finger protein 219 (ZNF219). For the mouse $Ca_V3.2$ promoter region, 239 different TF matrices were found with again the highest Z-score genome for Egr1 followed by ZF5 and brain and reproductive organ-expressed (BRE), whereas SP4, Egr1, and SP1 were found with the highest Z-scores calculated against all promoter regions. Finally, 203 TF matrices were found in the human $Ca_V3.2$ promoter region with nuclear respiratory factor 1 (NRF1), ZF5, and SP1 having the highest Z-score genome and SP1 (with two different matrices) and Egr1 with the highest Z-score promoter. Combining the overrepresentation values of rat, mouse, and human, we noticed that Egr1 was represented in the top Z-score lists of all three species (Table 1), pointing to a critical role of Egr1 for $Ca_V3.2$ promoter regulation.

Additional bioinformatic analysis of the $Ca_V3.2$ chromosomal region revealed that the overrepresentation of Egr1 was restricted to the evolutionary conserved promoter region (supplemental Fig. 1). Only one additional Egr1 binding site was found more than 1000 base pairs upstream of the identified $Ca_V3.2$ promoter region. Therefore, we decided to first examine if the cluster of Egr1 binding sites present in the conserved $Ca_V3.2$ promoter region mediates stimulation by Egr1.

Egr1 Strongly Activates $Ca_V3.2$ Promoter—To determine whether Egr1 actively regulates $Ca_V3.2$ promoter activity, an expression vector for Egr1 (24) was transfected into NG108-15 cells. Although NG108-15 cells express Egr1 constitutively (Fig. 3*A*), quantitative RT-PCR revealed significantly higher levels of $Ca_V3.2$ mRNA levels in Egr1-overexpressing NG108-15 cells

TABLE 1
Overrepresented transcriptional binding sites in the *$Ca_V3.2$* promoter region of rat, mouse, and human

TF matrix	Number of matches	Z-Score genome	TF matrix	Number of matches	Z-score promoter
Rat (1464 bp)					
V$EGR1.02	19	54.57	V$EGR1.02	19	17.75
V$ZF5.02	18	40.46	V$SP4.01	19	16.86
V$SP4.01	19	38.68	V$ZNF219.01	22	15.72
V$SP1.02	17	38.57	V$ZF5.02	18	13.24
V$SP1.03	17	37.88	V$EGR1.03	17	12.81
O$BRE.01	4	28.86	V$SP1.03	17	12.58
V$CTCF.01	12	27.75	V$SP1.02	17	12.46
V$KLF7.01	10	27.15	V$ZF9.01	17	12.12
V$ZF9.01	17	26.79	V$SP1.01	18	11.27
V$HDBP1_2.01	6	25.68	V$GC.01	18	11.08
Mouse (1468 bp)					
V$EGR1.02	16	42.69	V$SP4.01	17	14.81
V$ZF5.02	16	40.17	V$EGR1.02	16	14.39
O$BRE.01	5	35.16	V$SP1.01	20	11.84
V$SP1.02	16	35.13	V$SP1.02	16	11.73
V$SP4.01	17	34.11	V$ZF5.02	16	11.65
V$SP1.03	15	32.91	V$GC.01	19	11.05
V$E2F.03	9	29.14	V$SP1.03	15	11.01
V$SP1.01	20	23.29	V$ZF9.01	16	10.90
V$ZF9.01	16	23.18	V$ZNF219.01	18	10.72
V$CTCF.01	11	22.15	V$E2F.03	9	9.59
Human (1597 bp)					
V$NRF1.01	31	76.50	V$SP1.01	39	21.29
V$ZF5.02	27	75.03	V$SP1.03	35	21.16
V$SP1.03	35	67.26	V$EGR1.02	28	19.48
V$EGR1.02	28	65.48	V$SP4.01	26	18.77
V$SP1.02	31	59.53	V$SP1.02	31	18.75
V$CTCF.01	29	56.18	V$ZF9.01	31	18.43
V$SP1.01	39	56.10	V$CTCF.01	29	18.20
V$HDBP1_2.01	20	55.70	V$NRF1.01	31	17.65
V$SP4.01	26	51.35	V$ZF5.02	27	17.37
V$ZF9.01	31	49.60	V$ZNF219.01	27	16.71

(1.6-fold up-regulation; $p = 0.0054$; Fig. 3*B*). In addition, overexpression of Egr1 also induced a robust up-regulation of luciferase activity of the full-length *$Ca_V3.2$*−1426 reporter construct ($p \leq 0.001$), whereas no up-regulation was observed for the promoterless pGL3 control plasmid (Fig. 3*C*). These results show that the cluster of Egr1 binding sites present in the 1426-bp fragment is sufficient to mediate stimulation of *$Ca_V3.2$* transcription by Egr1.

Egr1 expression in cells is highly dynamic and can be altered by various stimuli. To examine the relationship between Egr1 levels in the cell and the transcriptional activity of the *$Ca_V3.2$* promoter, we transfected NG108-15 cells with increasing amounts of Egr1 (2.5–75 ng/well) and determined the respective *$Ca_V3.2$* luciferase activity. We observed that *$Ca_V3.2$* activity was augmented as a function of gradually increasing Egr1 concentrations (Fig. 3*D*), with a plateau phase reached at ~20 ng/well Egr1. Higher amounts of Egr1 resulted in a decrease in *$Ca_V3.2$* promoter activity, indicating a saturation of Egr1-induced *$Ca_V3.2$* promoter activity at ~20 ng/well.

Egr1 Increases Functional Expression of T-type Ca^{2+} Channels—To examine whether increased neuronal Egr1 augments T-type Ca^{2+} channels on a functional level, NG108-15 cells were transfected with Egr1, and Ca^{2+} currents were recorded in whole cell condition. Ca^{2+} currents were isolated pharmacologically by blocking Na^+ and K^+ conductance (see "Experimental Procedures"). From a holding potential of −80 mV, Ca^{2+} currents were elicited by a voltage step to −10 mV (Fig. 3*E*). In Egr1-transfected cells, T-type currents were strongly increased (Fig. 3*E*, compare *left* and *right current traces*). On average, the magnitude of T-type currents was increased more than 2-fold in Egr1-transfected cells (Fig. 3*F*, 35.5 ± 4.5 pA, $n = 13$, *versus* 109.3 ± 14.2 pA, $n = 13$, in control and Egr1 transfected neurons respectively, $p \leq 0.001$), indicating a major functional role for Egr1 in regulating I_{CaT}. The recorded currents can be attributed to $Ca_V3.2$, as they were largely blocked by application of 100 μM Ni^{2+} (Fig. 3*F*, *gray traces*, $n = 6$ *versus* $n = 5$ in control and Egr1-transfected neurons).

Specific Binding of Egr1 to $Ca_V3.2$ Promoter—To determine the region of the *$Ca_V3.2$* promoter involved in the strong Egr1-mediated up-regulation, Egr1 was cotransfected with the *$Ca_V3.2$* reporter deletion constructs. Overexpression of Egr1 showed a gradual decrease in luciferase activity for the deletion fragments, with the largest luciferase activity for the full-length *$Ca_V3.2$*−1426 reporter fragment (10-fold up-regulation; $p \leq 0.001$) and the lowest luciferase activity for the smallest *$Ca_V3.2$*−105 fragment (1.4-fold up-regulation; $p = 0.0026$) (Fig. 4*A*). These results imply that Egr1 effectively up-regulates promoter activity of *$Ca_V3.2$* reporter constructs mainly via sequences located more upstream in the *$Ca_V3.2$* promoter region.

To further support our hypothesis that the *$Ca_V3.2$* promoter could be a target of Egr1 and to further pinpoint the region responsible for Egr1-induced *$Ca_V3.2$* up-regulation, we performed ChIP experiments. 18 putative Egr1 responsive elements (EREs) are located within the *$Ca_V3.2$* promoter region (supplemental Fig. 1 and 2 and Fig. 4*B*), of which only the first two EREs are located within the full-length *$Ca_V3.2$*−1426 reporter construct. Because the up-regulation in luciferase activity after Egr1 stimulation was significantly different

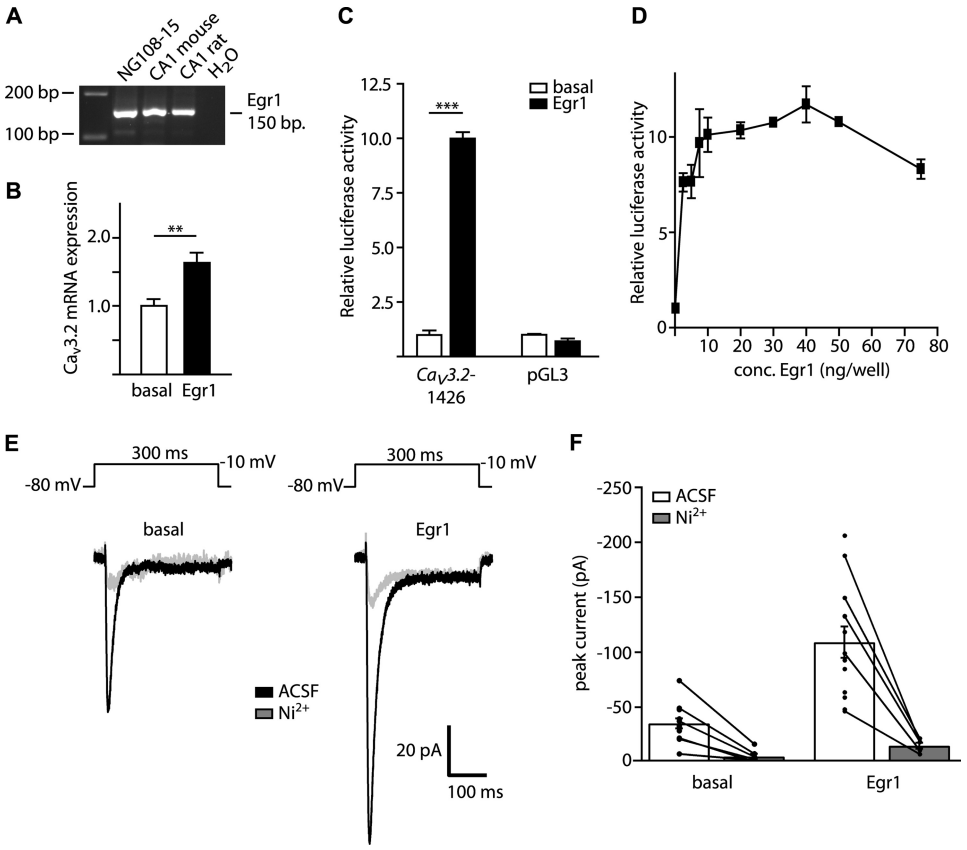

FIGURE 3. **Egr1 activates the $Ca_V3.2$ promoter and increases functional expression of $Ca_V3.2$.** *A*, shown is Egr1 mRNA expression in NG108-15 cells and mouse/rat hippocampal CA1 region. *B*, quantitative RT-PCR on RNA extracted from empty vector (basal) and Egr1-overexpressed NG108-15 cells (*t* test; **, $p \leq 0.01$; $n = 5$) is shown. *C*, luciferase activity of the full-length $Ca_V3.2-1426$ reporter construct and the promoterless pGL3 vector after stimulation with 25 ng Egr1 in NG108-15 cells (*t* test; ***, $p \leq 0.001$; $n = 4$) is shown. *D*, shown is the relationship between the concentration of transfected Egr1 (ranging from 0 to 75 ng/well) and the transcriptional activity of the $Ca_V3.2-1426$ luciferase construct. *E*, Ca^{2+} currents were elicited with a voltage step from −80 to −10 mV (*upper part*). Representative current traces show an increased amplitude in Egr1 transfected cells (*black trace right*) compared with controls (*black trace left*). The recorded currents were largely blocked by application of 100 μM Ni^{2+} (*gray traces*). *F*, average of the transient Ca^{2+} current of all cells for control cells (-35.5 ± 4.5 pA, $n = 13$) and Egr1-transfected cells (−109.3 ± 14.2 pA, $n = 13$) display a significant up-regulation of T-type Ca^{2+} currents after Egr1 transfection (*t* test; ***, $p \leq 0.001$). Average of the transient currents after application of 100 μM Ni^{2+} showed the large amplitude reduction in all recorded cells (basal, 5.5 ± 2.4 pA, $n = 5$; Egr1-transfected, 15,3 ± 2.7 pA, $n = 5$). *ACSF*, artificial cerebrospinal fluid control-solution.

between full-length $Ca_V3.2-1426$ and $Ca_V3.2-1188$ (Fig. 4*A*), we hypothesized that the two most upstream EREs have the highest binding efficacy.

For the ChIP experiments, NG108-15 cells were transfected with Egr1 and compared with empty vector-transfected control cells. We examined binding of Egr1 to the $Ca_V3.2$ promoter by using an Egr1-specific antibody. A rabbit-IgG no-antibody reaction served as a negative control, and three different primer pairs were used to cover the $Ca_V3.2$ promoter region. Intriguingly, the most upstream ChIP fragment 3 of the $Ca_V3.2$ promoter (containing the two predicted upstream EREs; Fig. 4*B*) was strongly enriched after immunoprecipitation with anti-Egr1 (Fig. 4, *C* and *D*). No significant difference was observed for the ChIP fragments 1 and 2. These observations indicate that Egr1 binds to the $Ca_V3.2$ promoter in neural cells and suggest that Egr1 overexpression leads to $Ca_V3.2$ promoter activation by the use of the upstream EREs.

REST Binds $Ca_V3.2$ Gene in NG108-15 Cells—Next, we examined whether Egr1-induced up-regulation of $Ca_V3.2$ can be counteracted by inhibitory elements located in the $Ca_V3.2$ gene. One repressor element known to be involved in $Ca_V3.2$ transcriptional regulation is REST. The $Ca_V3.2$ gene contains a highly conserved binding site for REST (RE-1) in its first intron (Fig. 5*A*), and this binding site has been reported capable of effectively binding REST (16, 18). To investigate whether Egr1-induced up-regulation of $Ca_V3.2$ could be counteracted by REST, we first analyzed NG108-15 cells for their endogenous REST mRNA expression. RT-PCR analysis revealed a clear band for the NG108-15 sample using primers against full-length REST and the truncated REST4 variant (Fig. 5*B*), indicating sufficient REST expression in the neuronal cell line.

Next, we cloned the $Ca_V3.2$ RE-1 sequence downstream of the full-length $Ca_V3.2-1426$ luciferase reporter construct (Fig. 5*C*) and compared basal activity of the $Ca_V3.2-1426$-REST reporter gene with the basal activity of $Ca_V3.2-1426$. We found no difference in basal activity for the two reporter constructs (Fig. 5*D*). In addition, overexpression of REST (25) or a dominant-negative variant of REST (RESTdN (26)) did not show an effect on the basal activity of any of the two reporter genes (Fig. 5*E*), suggesting no significant effect of REST on the $Ca_V3.2$ promoter fragment under study in naïve NG108-15 cells.

To investigate whether REST indeed binds the RE-1 site of the $Ca_V3.2$ gene, ChIP experiments on NG108-15 lysates were

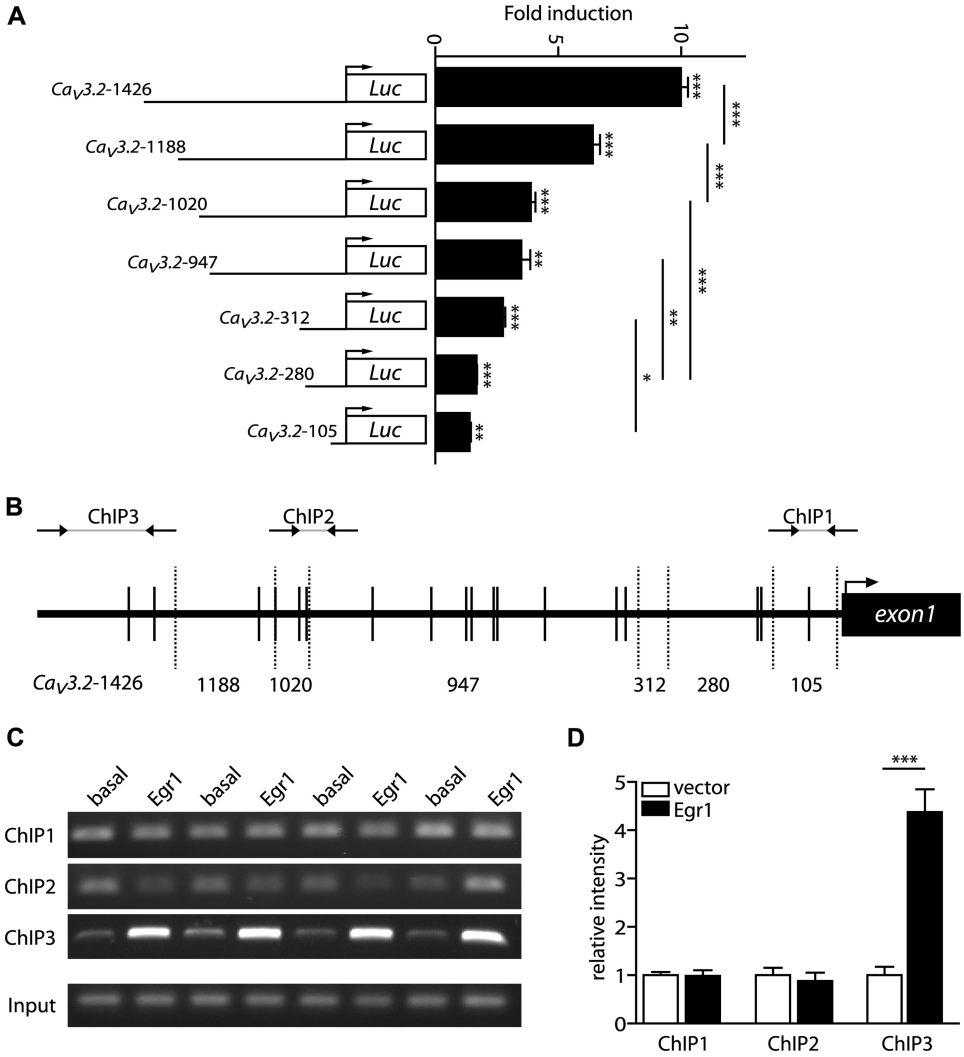

FIGURE 4. **Egr1 binds the upstream *$Ca_V3.2$* promoter.** *A*, luciferase activity of the *$Ca_V3.2$* promoter deletion fragments after overexpression with Egr1 is shown. Deletion of the upstream nucleotides of the *$Ca_V3.2$* promoter region gradually decreases the luciferase activity after Egr1 stimulation (one-way ANOVA: *, $p \leq 0.05$; **, $p \leq 0.01$; ***, $p \leq 0.001$; $n \geq 3$). *B*, shown is a schematic representation of the rat *$Ca_V3.2$* promoter and the amplicons used in the ChIP assay. *Vertical black bars* represent predicted Egr1 binding sites; *vertical dashed lines* represent the borders of the *$Ca_V3.2$* promoter deletion fragments. Three ChIP PCR assays were designed spanning the *$Ca_V3.2$* promoter region (ChIP1, -2, and -3). *C*, PCR analysis of the three ChIP products is shown. Binding efficiency of Egr1 to the *$Ca_V3.2$* promoter region was determined in empty vector (basal) and Egr1-overexpressing (*Egr1*) cells. *D*, quantification of the ChIP experiment under the two conditions indicated substantial binding of Egr1 at the *$Ca_V3.2$* promoter region covered by ChIP3 (*t* test: ***, $p \leq 0.001$; $n = 4$).

performed using a REST antibody. In both basal and REST-overexpressing NG108-15 cells, PCR amplicons were obtained, indicating efficient binding of REST to the *$Ca_V3.2$* gene (Fig. 5*F*). Nevertheless, no difference in binding efficiency was observed between immunoprecipitates generated from basal NG108-15 lysates and lysates from REST-overexpressing cells (Fig. 5*G*). Thus, under unstimulated conditions, up-regulation of REST has no effect on *$Ca_V3.2$* promoter binding and *$Ca_V3.2$* expression.

REST Potently Counteracts Egr1-induced $Ca_V3.2$ Activation—Next, we examined the effect of increasing REST concentrations on the *$Ca_V3.2$* promoter activity of Egr1-stimulated NG108-15 cells. Cotransfection of Egr1 (25 ng/well) and REST resulted in a significant repression of the *$Ca_V3.2$*−1426-REST reporter gene when cells were treated with more than 100 ng/well REST (Fig. 6*A*). No down-regulation of Egr1-induced *$Ca_V3.2$* promoter activity was observed in transfected cells harboring *$Ca_V3.2$*−1426 lacking a REST binding site (Fig. 6*B*). In addition, RESTdN did not have an effect on any of the two promoter constructs. Intriguingly, these results indicate that recruitment of REST to the RE-1 site of the *$Ca_V3.2$* promoter effectively represses Egr1-induced *$Ca_V3.2$* expression.

Egr1 and REST Bind $Ca_V3.2$ Promoter in Vivo—To analyze whether the above described effects in NG108-15 cells have any physiological relevance *in vivo*, ChIP analyses using anti-Egr1 and anti-REST antibodies were carried out on brain tissues. Because expression levels of the two target genes *Egr1* and *REST* are relatively high in hippocampal tissue (Figs. 3*A* and 5*B*), we selected mouse hippocampi for our experiments. Anti-Egr1 and anti-REST hippocampal immunoprecipitates were analyzed for their binding to the *$Ca_V3.2$* gene. Primers specific to the *$Ca_V3.2$* promoter region (Fig. 4*B*) yielded PCR amplicons from the anti-Egr1 chromatin (Fig. 7*A*). In addition, PCR amplicons were also obtained from anti-REST immunoprecipitates when using primers specific for the RE-1 sequence of the *$Ca_V3.2$* gene (Fig. 7*A*). Hence, consistent with the finding that

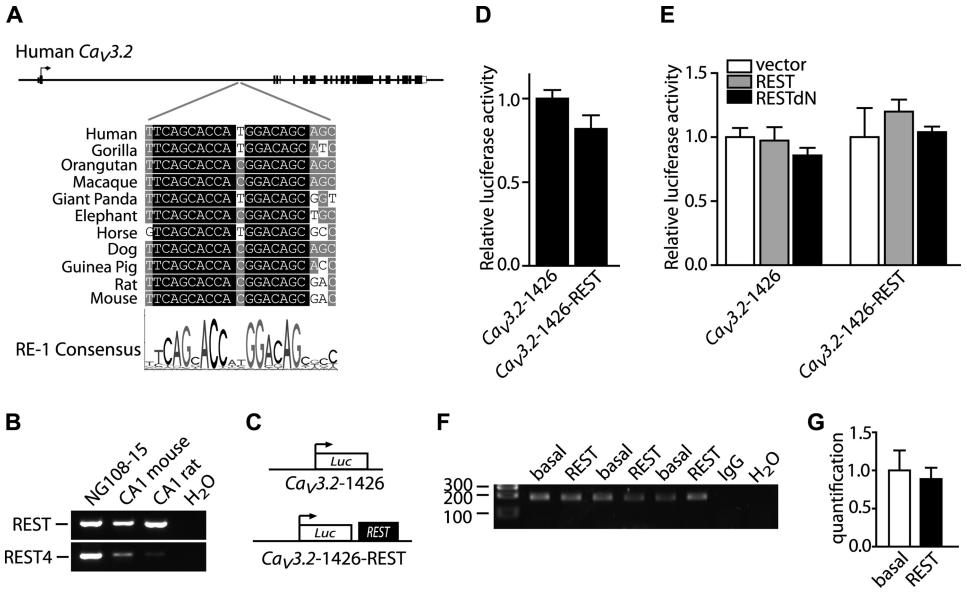

FIGURE 5. **The transcriptional repressor REST binds the $Ca_V3.2$ gene in NG108-15 cells.** *A*, shown is a graphic representation of the rat $Ca_V3.2$ gene with exons represented by *black boxes*. Conservation analysis of the RE-1 sequence located in intron 1 of the $Ca_V3.2$ gene is given for a number of vertebrates, with the RE-1 "Genomatix" consensus matrix included below. Sequences were aligned using Vector NTI (9.0) with default parameters. *B*, REST mRNA expression in NG108-15 cells and mouse/rat hippocampal CA1 region is shown. *C*, shown is a schematic representation of the $Ca_V3.2$−1426 and $Ca_V3.2$−1426-REST luciferase reporter constructs. *D*, basal activities of the full-length $Ca_V3.2$−1426 and $Ca_V3.2$−1426-REST reporter constructs in NG108-15 cells are similar, implying that the RE-1 sequence has no effect under control conditions. *E*, shown is luciferase activity of the $Ca_V3.2$−1426 and $Ca_V3.2$−1426-REST reporter constructs after overexpression of REST (25 ng) *versus* a dominant-negative variant of REST (RESTdN; 25 ng). *F*, ChIP analysis of REST binding to the $Ca_V3.2$ gene is shown. PCR amplicons were generated of anti-REST ChIP immunoprecipitates from empty vector (*basal*) and REST-overexpressing (*REST*) NG108-15 cells. A rabbit-IgG immunoprecipitate was used as negative control. *G*, quantification of the anti-REST ChIP analysis is shown.

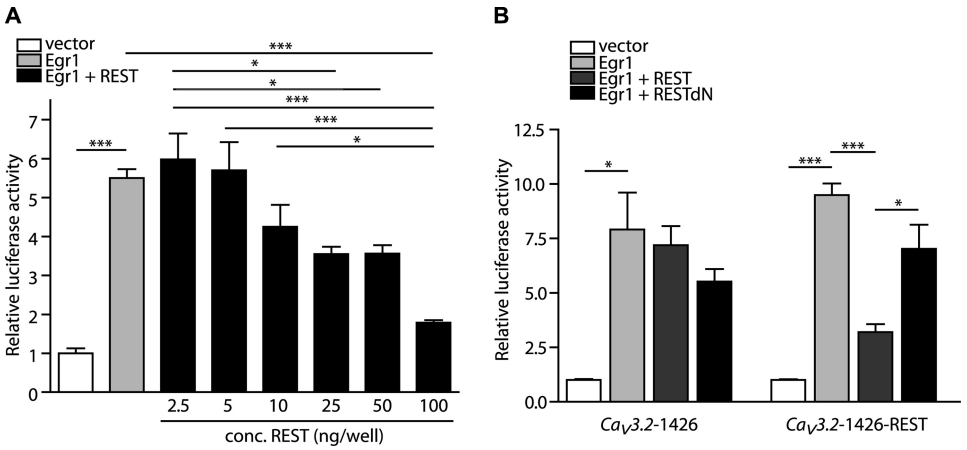

FIGURE 6. **Egr1 induced $Ca_V3.2$ promoter activity is counteracted by REST.** *A*, NG108-15 cells transfected with the $Ca_V3.2$−1426-REST reporter construct, Egr1 (25 ng/well), and increasing concentrations of the REST plasmid (2.5–100 ng/well) are shown. Increasing amounts of REST resulted in a gradual decrease in $Ca_V3.2$ promoter activity (one-way ANOVA: *, $p \leq 0.05$; ***, $p \leq 0.001$; $n \geq 3$). *B*, shown is the two promoter-luciferase reporter constructs ($Ca_V3.2$−1426 and $Ca_V3.2$−1426-REST) stimulated with 25 ng of Egr1, 25 ng of REST, and 25 ng of RESTdN. Simultaneous expression of Egr1 and REST does prevent Egr1-induced activation of $Ca_V3.2$−1426-REST but not $Ca_V3.2$−1426 (one-way ANOVA: *, $p \leq 0.05$; ***, $p \leq 0.001$; $n \geq 3$).

Egr1 and REST can bind the $Ca_V3.2$ gene in NG108-15 cells, ChIP analysis of mouse hippocampi revealed that Egr1 and REST also bind the $Ca_V3.2$ gene *in vivo*.

Overexpression of Egr1 Increases $Ca_V3.2$ Expression in Vivo—Finally, we investigated whether the Egr1-induced up-regulation of $Ca_V3.2$ also occurs *in vivo*. Egr1 overexpression was accomplished by stereotaxical delivery of an AAV encoding the Egr1 protein in the hippocampus of adult mice. Two weeks after injection, hippocampal $Ca_V3.2$ and Egr1 mRNA expression levels were measured. We observed a significant up-regulation of Egr1 mRNA expression after rAAV-Egr1 transduction, indicating efficient rAAV infection in the hippocampus (Fig. 7*B*, *left panel*). Intriguingly, a significant up-regulation of $Ca_V3.2$ expression was also observed after infection with rAAV-Egr1 (Fig. 7*B*, *right panel*). Collectively, these data indicate that Egr1 can increase $Ca_V3.2$ expression not only in cultured cells but also in brain tissue.

DISCUSSION

Here, we have defined a regulatory element in the upstream $Ca_V3.2$ promoter that mediates activation of $Ca_V3.2$ transcription by Egr1. Stimulation of the $Ca_V3.2$ promoter by Egr1 thereby leads to an increase of I_{CaT}. Furthermore, we observed that Egr1-mediated promoter activation

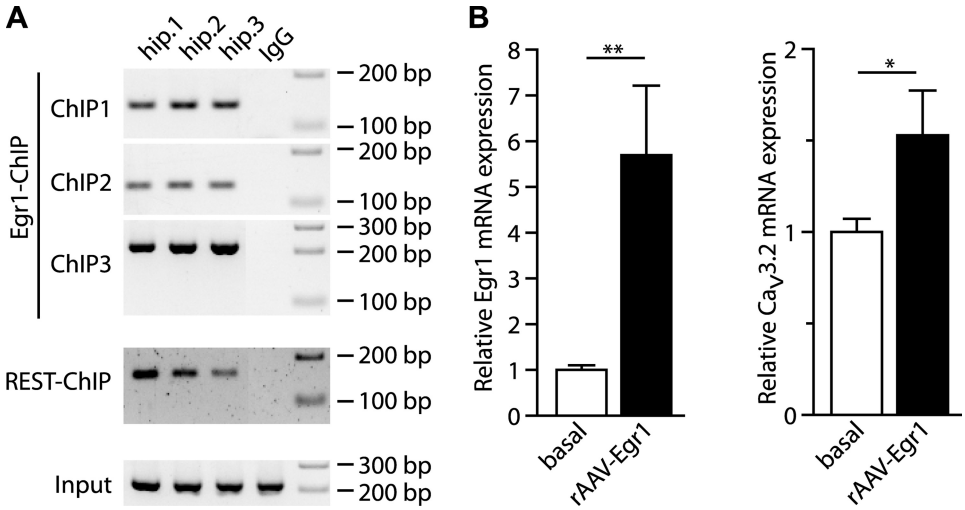

FIGURE 7. **Egr1 and REST bind the *$Ca_V3.2$* promoter *in vivo*.** *A*, ChIP analysis of Egr1 and REST in mouse hippocampi is shown. Binding efficiency of Egr1 and REST to the *$Ca_V3.2$* gene was tested using four primer sets spanning the *$Ca_V3.2$* promoter region (*Egr1-ChIP*) and the RE-1 binding site in the first intron of the *$Ca_V3.2$* gene (*REST-ChIP*). Notably, PCR amplicons were obtained for all four primer sets, indicating efficient Egr1 and REST binding to the *$Ca_V3.2$* gene. A rabbit-IgG reaction served as negative control. *B*, shown is quantitative RT-PCR on RNA extracted from total hippocampi isolated from control (basal; $n = 7$) and rAAV-Egr1-injected ($n = 4$) mice. Egr1 and $Ca_V3.2$ mRNA expression levels were measured 14 days after injection, with β-actin as reference gene (*t* test: *$p \leq 0.05$; **, ≤ 0.01).

can be effectively counteracted by binding of the transcriptional repressor REST to the *$Ca_V3.2$* gene (Fig. 8). In contrast to short term modulatory effects on I_{CaT} (for review, see Ref. 27), the mechanisms, we observed here, are well suited for prolonged dynamic regulation of neuronal and cardiac Ca^{2+}-homeostasis and discharge behavior.

Our bioinformatic analyses revealed a striking accumulation of adjacent binding sites for Egr1 in the upstream *$Ca_V3.2$* promoter region. Such "homotypic" TF binding clusters are a widespread genomic feature of higher eukaryotes (28) and may be utilized to control gene expression via sophisticated regulatory mechanisms such as high affinity cooperative binding of the corresponding TF (29). In general, cooperative TF binding can be translated into on/off transcriptional responses, regulating the functional state of the corresponding gene, namely, active or inactive. In contrast, non-cooperative TF binding does not switch between a digital (on/off) transcriptional response but results in a more gradual transcriptional activation (30). Our ChIP data reveal Egr1 binding to all Egr1 binding sites of the *$Ca_V3.2$* promoter under basal conditions, indicating a cooperative mechanism of *$Ca_V3.2$* transcriptional regulation. However, in the presence of increased Egr1 levels, augmented Egr1 binding occurred only at the two most upstream Egr1 binding sites, suggesting these binding sites to be of importance for strong stimulus-induced *$Ca_V3.2$* up-regulation.

Egr1 is a zinc finger transcription factor and belongs to a larger family of early response genes that also include *Egr2, Egr3, Egr4,* and Wilms tumor 1 (*Wt1*). Egr1 is rapidly and transiently induced by a variety of stimuli, including serum, growth factors, mechanical injury, stress, and ischemia and has important roles in the regulation of cell growth, differentiation, development, and apoptosis (31, 32). Upon induction, Egr1 can bind ERE consensus sequences to regulate expression of downstream target genes, such as fibronectin (*Fn1*), fibroblast growth factor 2 (*Fgf2*), synapsin I (*Syn1*), transforming growth factor, β1 (*Tgfβ1*), phosphatase and tensin homolog (*Pten*), and *p53* (for review, see Ref. 33). Furthermore, Egr1 has been reported to activate NGFI-A-binding protein 1 and 2 (*Nab1* and *Nab2*). Interestingly, both proteins also appear to be important regulators of Egr1-mediated transactivation (34–36). By binding to Egr1, Nab1 and Nab2 can strongly inhibit Egr1 activity. Nab1 and Nab2 are also expressed in NG108-15 cells, but only Nab2 is significantly up-regulated after Egr1 stimulation.[3] Congruently, Egr1 can regulate the induction of its own repressor Nab2, and can thus control its own transactivation efficiency in NG108-15 cells. This negative feedback loop provides a potential explanation for the saturation of Egr1-induced *$Ca_V3.2$* up-regulation when increasing levels of Egr1 are transfected (Fig. 3*D*).

Previous studies have shown that Egr1 and Sp1, for which there are also several potential binding sites within the *$Ca_V3.2$* promoter (Table 1), can generally compete for overlapping binding motifs (37, 38). Sp1 usually activates target promoter sequences but gives complex responses when in the presence of Egr-1 (39). Sp1 is also expressed in NG108-15 cells.[3] Therefore, Sp1 and Egr1 could recognize and competitively bind overlapping Sp1/Egr1 consensus sequences located in the *$Ca_V3.2$* promoter. Intriguingly, of the predicted Egr1 binding sites in the *$Ca_V3.2$* promoter (Fig. 4*B*), the two most upstream Egr1 binding sites, with the highest Egr1 binding efficiency in our ChIP experiments, do not overlap with Sp1 consensus sequences (supplemental Fig. 1). This bioinformatic finding together with our data suggest that the two upstream Egr1 binding sites that are critical for a dose-dependent *$Ca_V3.2$* promoter control by Egr1 are exclusively controlled by Egr1 and not by Sp1.

We found that the transcriptional repressor REST counteracts the stimulatory effect of Egr1 on the *$Ca_V3.2$* promoter. The *$Ca_V3.2$* gene contains a highly conserved RE-1 that can interact with REST. Originally, REST was identified to be important for

[3] K. M. J. van Loo, C. Schaub, K. Pernhorst, Y. Yaari, H. Beck, S. Schoch, and A. J. Becker, unpublished observations.

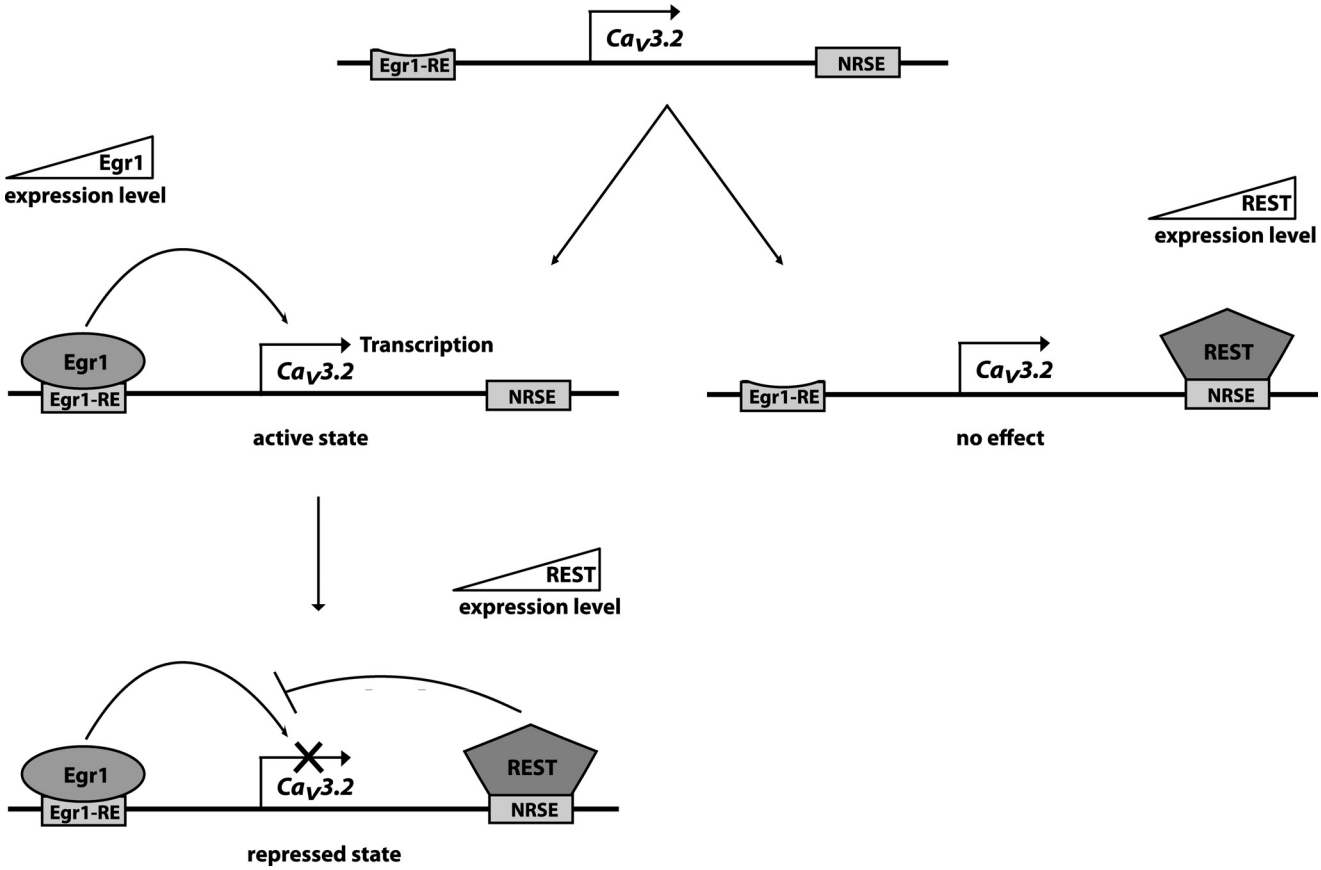

FIGURE 8. **Model of $Ca_V3.2$ promoter regulation by Egr1 and REST.** Increases in Egr1 levels result in the activation of the $Ca_V3.2$ promoter (*active state*). Subsequent addition of REST can repress the activated $Ca_V3.2$ promoter (*repressed state*). REST overexpression alone does not influence $Ca_V3.2$ promoter activity (*no effect*). *NRSE*, neuron-restrictive silencer element.

the silencing of neuronal-specific genes in non-neuronal cells (40). Nevertheless, REST also has a functional role within the nervous system by regulating expression of several target genes, including *Syn1*, synaptophysin (*Syp*), the type II sodium channel genes (*Scn2A* and *Scn2B*), and the genes encoding the potassium channel subunits Kv7.2 and Kv7.3 (*Kcnq2* and *Kcnq3*) (41, 42). Recently a large scale chromatin immunoprecipitation assay (ChIPSeq) was performed to build a high resolution interactome map for REST (43). Here, $Ca_V3.2$ was identified as a REST-responsive gene as well as were other members of the voltage-dependent calcium channel subunit family (*e.g. Cacna1a*, *Cacna1b*, *cacna1e* and *cacna2d2*). In addition, many other ion channel genes were found positive for REST binding, including the sodium channels *Scn3b* and *Scn10a,* several potassium channels, and the hyperpolarization-activated cyclic nucleotide gated (*Hcn*) ion channel genes. In this context, REST may have a general role in coordinately regulating expression levels of ion channel proteins from different subfamilies, including the $Ca_V3.2$ gene.

REST did not repress the basal activity of the $Ca_V3.2$ promoter but strongly decreased Egr1-induced promoter activity. This observation suggests that because basal expression levels of $Ca_V3.2$ are low and the REST binding site in the $Ca_V3.2$ promoter is occupied during basal conditions (Figs. 5*F* and 7*A*), REST is involved in keeping basal $Ca_V3.2$ levels low. Therefore, an increase in REST levels cannot further down-regulate $Ca_V3.2$ expression. After Egr1 stimulation, REST binding to the RE-1 of the $Ca_V3.2$ gene might be relieved, resulting in augmented $Ca_V3.2$ expression levels. The Egr1-induced up-regulation can then only be repressed by higher REST availability. Therefore, REST may play an important role in keeping basal expression levels of $Ca_V3.2$ low before and after a transient activating stimulus. Transcriptional regulation by REST is even more complex due to the coexpression of REST4 (Fig. 5*B*). REST4, the truncated variant of REST that lacks the C-terminal zinc finger repressor domain can antagonize the action of full-length REST (44) and might thus interfere with REST-induced changes.

Transient transcriptional alterations of $Ca_V3.2$ relate to disorders with episodic onset of symptoms such as epileptic seizures and cardiac arrhythmias. The latter has been demonstrated to relate to the modulation of $Ca_V3.2$ transcription by REST (16, 18). Interestingly, highly dynamic changes of $Ca_V3.2$ expression have been observed in epileptogenesis after brain insults in thalamic as well as hippocampal principal neurons (14, 15). In hippocampal CA1 pyramidal cells, $Ca_V3.2$ mRNA is transiently up-regulated early in epileptogenesis that is triggered by an episode of status epilepticus (SE), leading to an increase in the propensity for intrinsic burst-firing (15, 45). Egr1 has been suggested as a critical factor for the establishment of long term neuronal plasticity in the hippocampal formation (46–48). Intriguingly, Egr1 expression is also strongly increased in hippocampal neurons after SE (49, 50). In addition, human twin studies showed a dysregulation of Egr1 mRNA expression in idiopathic absence epilepsies (51). In conjunction with our present data, these studies suggest that Egr1-

mediated transcriptional up-regulation of *$Ca_V3.2$* may be a mechanism generalizable to a number of CNS disorders.

Notably, *$Ca_V3.2$* mRNA peaks only transiently for 2 days after SE in CA1 pyramidal cells and afterward sharply returns to base-line levels (15). Neuronal REST expression is significantly up-regulated after global ischemia and epileptic insults (19–21, 52, 53). Extrapolating our present *in vitro* data to this condition, we suggest that augmented REST levels may be involved in *$Ca_V3.2$* repression 2 days after SE. A similar regulation by REST has been described for the hyperpolarization-activated cyclic nucleotide gated ion channel *Hcn1* after kainic acid-induced SE. The SE-induced up-regulation of REST represses *Hcn1* expression and the corresponding Hcn1-mediated currents (I_h) (53). REST, therefore, may play the role of a "central switch" in SE-induced channelopathies. The fact that strong expression of REST and its binding to the RE-1 of the *$Ca_V3.2$* gene counteracts Egr1-induced *$Ca_V3.2$* activation but does not interfere with the "basal" activity of the *$Ca_V3.2$* promoter raises the intriguing possibility that REST up-regulation may sharpen the temporal profile of *$Ca_V3.2$* up-regulation. This will depend to a great extent on the precise timing of Egr1 and subsequent REST induction. Further studies will be needed to analyze the effect of increased REST levels *in vivo*, *e.g.* after SE, on the *$Ca_V3.2$* transcriptional activity.

Interfering with a transcriptional complex that alters transcription of multiple disease-relevant genes represents a potential therapeutic approach. A detailed understanding of the responsible transcriptional regulatory mechanisms will allow for specific interference strategy. Therefore, our data showing that the *$Ca_V3.2$* promoter can be regulated by interplay of Egr1 and REST, whereby increases in cellular Egr1 activate the *$Ca_V3.2$* promoter while REST can counteract the Egr1-induced up-regulation, represents an important step in this direction.

Acknowledgments—We thank Gerald Thiel (Homburg, Germany) and Martin Schwarz (Heidelberg; Germany) for providing plasmids and Sabine Normann for excellent technical assistance.

REFERENCES

1. Bosch, M. A., Hou, J., Fang, Y., Kelly, M. J., and Rønnekleiv, O. K. (2009) 17β-Estradiol regulation of the mRNA expression of T-type calcium channel subunits. Role of estrogen receptor α and estrogen receptor β. *J. Comp. Neurol.* **512,** 347–358
2. Cribbs, L. (2010) T-type calcium channel expression and function in the diseased heart. *Channels* **4,** 447–452
3. McKay, B. E., McRory, J. E., Molineux, M. L., Hamid, J., Snutch, T. P., Zamponi, G. W., and Turner, R. W. (2006) Ca(V)3 T-type calcium channel isoforms differentially distribute to somatic and dendritic compartments in rat central neurons. *Eur. J. Neurosci.* **24,** 2581–2594
4. Molineux, M. L., McRory, J. E., McKay, B. E., Hamid, J., Mehaffey, W. H., Rehak, R., Snutch, T. P., Zamponi, G. W., and Turner, R. W. (2006) Specific T-type calcium channel isoforms are associated with distinct burst phenotypes in deep cerebellar nuclear neurons. *Proc. Natl. Acad. Sci. U.S.A.* **103,** 5555–5560
5. Leuranguer, V., Monteil, A., Bourinet, E., Dayanithi, G., and Nargeot, J. (2000) T-type calcium currents in rat cardiomyocytes during postnatal development. Contribution to hormone secretion. *Am. J. Physiol. Heart Circ. Physiol.* **279,** H2540–H2548
6. Chemin, J., Monteil, A., Perez-Reyes, E., Bourinet, E., Nargeot, J., and Lory, P. (2002) Specific contribution of human T-type calcium channel isotypes (α(1G), α (1H), and α (1I)) to neuronal excitability. *J. Physiol.* **540,** 3–14
7. Huguenard, J. R. (1996) Low threshold calcium currents in central nervous system neurons. *Annu. Rev. Physiol.* **58,** 329–348
8. Lee, J. H., Gomora, J. C., Cribbs, L. L., and Perez-Reyes, E. (1999) Nickel block of three cloned T-type calcium channels. Low concentrations selectively block α1H. *Biophys. J.* **77,** 3034–3042
9. Klöckner, U., Lee, J. H., Cribbs, L. L., Daud, A., Hescheler, J., Pereverzev, A., Perez-Reyes, E., and Schneider, T. (1999) Comparison of the Ca^{2+} currents induced by expression of three cloned α1 subunits, α1G, α1H, and α1I, of low voltage-activated T-type Ca^{2+} channels. *Eur. J. Neurosci.* **11,** 4171–4178
10. Lee, J. H., Daud, A. N., Cribbs, L. L., Lacerda, A. E., Pereverzev, A., Klöckner, U., Schneider, T., and Perez-Reyes, E. (1999) Cloning and expression of a novel member of the low voltage-activated T-type calcium channel family. *J Neurosci* **19,** 1912–1921
11. Khosravani, H., Bladen, C., Parker, D. B., Snutch, T. P., McRory, J. E., and Zamponi, G. W. (2005) Effects of Cav3.2 channel mutations linked to idiopathic generalized epilepsy. *Ann. Neurol.* **57,** 745–749
12. Khosravani, H., Altier, C., Simms, B., Hamming, K. S., Snutch, T. P., Mezeyova, J., McRory, J. E., and Zamponi, G. W. (2004) Gating effects of mutations in the Cav3.2 T-type calcium channel associated with childhood absence epilepsy. *J. Biol. Chem.* **279,** 9681–9684
13. Powell, K. L., Cain, S. M., Ng, C., Sirdesai, S., David, L. S., Kyi, M., Garcia, E., Tyson, J. R., Reid, C. A., Bahlo, M., Foote, S. J., Snutch, T. P., and O'Brien, T. J. (2009) A Cav3.2 T-type calcium channel point mutation has splice variant-specific effects on function and segregates with seizure expression in a polygenic rat model of absence epilepsy. *J. Neurosci.* **29,** 371–380
14. Graef, J. D., Nordskog, B. K., Wiggins, W. F., and Godwin, D. W. (2009) An acquired channelopathy involving thalamic T-type Ca^{2+} channels after status epilepticus. *J. Neurosci.* **29,** 4430–4441
15. Becker, A. J., Pitsch, J., Sochivko, D., Opitz, T., Staniek, M., Chen, C. C., Campbell, K. P., Schoch, S., Yaari, Y., and Beck, H. (2008) Transcriptional up-regulation of Cav3.2 mediates epileptogenesis in the pilocarpine model of epilepsy. *J. Neurosci.* **28,** 13341–13353
16. Kuwahara, K., Takano, M., and Nakao, K. (2005) Pathophysiological significance of T-type Ca^{2+} channels. Transcriptional regulation of T-type Ca^{2+} channel. Regulation of CACNA1H by neuron-restrictive silencer factor. *J. Pharmacol. Sci.* **99,** 211–213
17. Maturana, A., Lenglet, S., Python, M., Kuroda, S., and Rossier, M. F. (2009) Role of the T-type calcium channel CaV3.2 in the chronotropic action of corticosteroids in isolated rat ventricular myocytes. *Endocrinology* **150,** 3726–3734
18. Kuwahara, K., Saito, Y., Takano, M., Arai, Y., Yasuno, S., Nakagawa, Y., Takahashi, N., Adachi, Y., Takemura, G., Horie, M., Miyamoto, Y., Morisaki, T., Kuratomi, S., Noma, A., Fujiwara, H., Yoshimasa, Y., Kinoshita, H., Kawakami, R., Kishimoto, I., Nakanishi, M., Usami, S., Saito, Y., Harada, M., and Nakao, K. (2003) NRSF regulates the fetal cardiac gene program and maintains normal cardiac structure and function. *EMBO J.* **22,** 6310–6321
19. Spencer, E. M., Chandler, K. E., Haddley, K., Howard, M. R., Hughes, D., Belyaev, N. D., Coulson, J. M., Stewart, J. P., Buckley, N. J., Kipar, A., Walker, M. C., and Quinn, J. P. (2006) Regulation and role of REST and REST4 variants in modulation of gene expression in *in vivo* and *in vitro* in epilepsy models. *Neurobiol. Dis.* **24,** 41–52
20. Palm, K., Belluardo, N., Metsis, M., and Timmusk, T. (1998) Neuronal expression of zinc finger transcription factor REST/NRSF/XBR gene. *J. Neurosci.* **18,** 1280–1296
21. Calderone, A., Jover, T., Noh, K. M., Tanaka, H., Yokota, H., Lin, Y., Grooms, S. Y., Regis, R., Bennett, M. V., and Zukin, R. S. (2003) Ischemic insults derepress the gene silencer REST in neurons destined to die. *J. Neurosci.* **23,** 2112–2121
22. Uchida, H., Ma, L., and Ueda, H. (2010) Epigenetic gene silencing underlies C-fiber dysfunctions in neuropathic pain. *J. Neurosci.* **30,** 4806–4814
23. Down, T. A., and Hubbard, T. J. (2002) Computational detection and location of transcription start sites in mammalian genomic DNA. *Genome Res.* **12,** 458–461
24. Thiel, G., Schoch, S., and Petersohn, D. (1994) Regulation of synapsin I

gene expression by the zinc finger transcription factor zif268/egr-1. *J. Biol. Chem.* **269,** 15294–15301
25. Thiel, G., Lietz, M., and Cramer, M. (1998) Biological activity and modular structure of RE-1-silencing transcription factor (REST), a repressor of neuronal genes. *J. Biol. Chem.* **273,** 26891–26899
26. Lietz, M., Bach, K., and Thiel, G. (2001) Biological activity of RE-1 silencing transcription factor (REST) toward distinct transcriptional activators. *Eur. J. Neurosci.* **14,** 1303–1312
27. Chemin, J., Traboulsie, A., and Lory, P. (2006) Molecular pathways underlying the modulation of T-type calcium channels by neurotransmitters and hormones. *Cell Calcium* **40,** 121–134
28. Lifanov, A. P., Makeev, V. J., Nazina, A. G., and Papatsenko, D. A. (2003) Homotypic regulatory clusters in *Drosophila*. *Genome Res.* **13,** 579–588
29. Hertel, K. J., Lynch, K. W., and Maniatis, T. (1997) Common themes in the function of transcription and splicing enhancers. *Curr. Opin. Cell Biol.* **9,** 350–357
30. Giorgetti, L., Siggers, T., Tiana, G., Caprara, G., Notarbartolo, S., Corona, T., Pasparakis, M., Milani, P., Bulyk, M. L., and Natoli, G. (2010) Noncooperative interactions between transcription factors and clustered DNA binding sites enable graded transcriptional responses to environmental inputs. *Mol. Cell* **37,** 418–428
31. Sukhatme, V. P., Cao, X. M., Chang, L. C., Tsai-Morris, C. H., Stamenkovich, D., Ferreira, P. C., Cohen, D. R., Edwards, S. A., Shows, T. B., and Curran, T. (1988) A zinc finger-encoding gene coregulated with c-fos during growth and differentiation and after cellular depolarization. *Cell* **53,** 37–43
32. Liu, C., Rangnekar, V. M., Adamson, E., and Mercola, D. (1998) Suppression of growth and transformation and induction of apoptosis by EGR-1. *Cancer Gene Ther.* **5,** 3–28
33. Baron, V., Adamson, E. D., Calogero, A., Ragona, G., and Mercola, D. (2006) The transcription factor Egr1 is a direct regulator of multiple tumor suppressors including TGFβ1, PTEN, p53, and fibronectin. *Cancer Gene Ther.* **13,** 115–124
34. Svaren, J., Sevetson, B. R., Apel, E. D., Zimonjic, D. B., Popescu, N. C., and Milbrandt, J. (1996) NAB2, a corepressor of NGFI-A (Egr-1) and Krox20, is induced by proliferative and differentiative stimuli. *Mol. Cell. Biol.* **16,** 3545–3553
35. Russo, M. W., Sevetson, B. R., and Milbrandt, J. (1995) Identification of NAB1, a repressor of NGFI-A- and Krox20-mediated transcription. *Proc. Natl. Acad. Sci. U.S.A.* **92,** 6873–6877
36. Kumbrink, J., Gerlinger, M., and Johnson, J. P. (2005) Egr-1 induces the expression of its corepressor nab2 by activation of the nab2 promoter thereby establishing a negative feedback loop. *J. Biol. Chem.* **280,** 42785–42793
37. Ackerman, S. L., Minden, A. G., Williams, G. T., Bobonis, C., and Yeung, C. Y. (1991) Functional significance of an overlapping consensus binding motif for Sp1 and Zif268 in the murine adenosine deaminase gene promoter. *Proc. Natl. Acad. Sci. U.S.A.* **88,** 7523–7527
38. Gannon, A. M., Turner, E. C., Reid, H. M., and Kinsella, B. T. (2009) Regulated expression of the α isoform of the human thromboxane A2 receptor during megakaryocyte differentiation. A coordinated role for WT1, Egr1, and Sp1. *J. Mol. Biol.* **394,** 29–45
39. Huang, R. P., Fan, Y., Ni, Z., Mercola, D., and Adamson, E. D. (1997) Reciprocal modulation between Sp1 and Egr-1. *J. Cell. Biochem.* **66,** 489–499
40. Schoenherr, C. J., and Anderson, D. J. (1995) The neuron-restrictive silencer factor (NRSF). A coordinate repressor of multiple neuron-specific genes. *Science* **267,** 1360–1363
41. Mucha, M., Ooi, L., Linley, J. E., Mordaka, P., Dalle, C., Robertson, B., Gamper, N., and Wood, I. C. (2010) Transcriptional control of KCNQ channel genes and the regulation of neuronal excitability. *J. Neurosci.* **30,** 13235–13245
42. Schoenherr, C. J., Paquette, A. J., and Anderson, D. J. (1996) Identification of potential target genes for the neuron-restrictive silencer factor. *Proc. Natl. Acad. Sci. U.S.A.* **93,** 9881–9886
43. Johnson, D. S., Mortazavi, A., Myers, R. M., and Wold, B. (2007) Genome-wide mapping of *in vivo* protein-DNA interactions. *Science* **316,** 1497–1502
44. Shimojo, M., Paquette, A. J., Anderson, D. J., and Hersh, L. B. (1999) Protein kinase A regulates cholinergic gene expression in PC12 cells. REST4 silences the silencing activity of neuron-restrictive silencer factor/REST. *Mol. Cell. Biol.* **19,** 6788–6795
45. Su, H., Sochivko, D., Becker, A., Chen, J., Jiang, Y., Yaari, Y., and Beck, H. (2002) Up-regulation of a T-type Ca^{2+} channel causes a long-lasting modification of neuronal firing mode after status epilepticus. *J. Neurosci.* **22,** 3645–3655
46. Heynen, A. J., and Bear, M. F. (2001) Long term potentiation of thalamocortical transmission in the adult visual cortex *in vivo*. *J. Neurosci.* **21,** 9801–9813
47. Wei, F., Xu, Z. C., Qu, Z., Milbrandt, J., and Zhuo, M. (2000) Role of EGR1 in hippocampal synaptic enhancement induced by tetanic stimulation and amputation. *J. Cell Biol.* **149,** 1325–1334
48. McDade, D. M., Conway, A. M., James, A. B., and Morris, B. J. (2009) Activity-dependent gene transcription as a long term influence on receptor signaling. *Biochem. Soc. Trans.* **37,** 1375–1377
49. Hughes, P., and Dragunow, M. (1994) Activation of pirenzepine-sensitive muscarinic receptors induces a specific pattern of immediate-early gene expression in rat brain neurons. *Brain Res. Mol. Brain Res.* **24,** 166–178
50. Beckmann, A. M., Davidson, M. S., Goodenough, S., and Wilce, P. A. (1997) Differential expression of Egr-1-like DNA binding activities in the naive rat brain and after excitatory stimulation. *J. Neurochem.* **69,** 2227–2237
51. Helbig, I., Matigian, N. A., Vadlamudi, L., Lawrence, K. M., Bayly, M. A., Bain, S. M., Diyagama, D., Scheffer, I. E., Mulley, J. C., Holloway, A. J., Dibbens, L. M., Berkovic, S. F., and Hayward, N. K. (2008) Gene expression analysis in absence epilepsy using a monozygotic twin design. *Epilepsia* **49,** 1546–1554
52. Garriga-Canut, M., Schoenike, B., Qazi, R., Bergendahl, K., Daley, T. J., Pfender, R. M., Morrison, J. F., Ockuly, J., Stafstrom, C., Sutula, T., and Roopra, A. (2006) 2-Deoxy-D-glucose reduces epilepsy progression by NRSF-CtBP-dependent metabolic regulation of chromatin structure. *Nat. Neurosci.* **9,** 1382–1387
53. McClelland, S., Flynn, C., Dubé, C., Richichi, C., Zha, Q., Ghestem, A., Esclapez, M., Bernard, C., and Baram, T. Z. (2011) Neuron-restrictive silencer factor-mediated hyperpolarization-activated cyclic nucleotide gated channelopathy in experimental temporal lobe epilepsy. *Ann. Neurol.* **70,** 454–464